

Figure 28. Weight loss assembly at the Long Term Corrosion Test Facility (LTCTF).²⁹

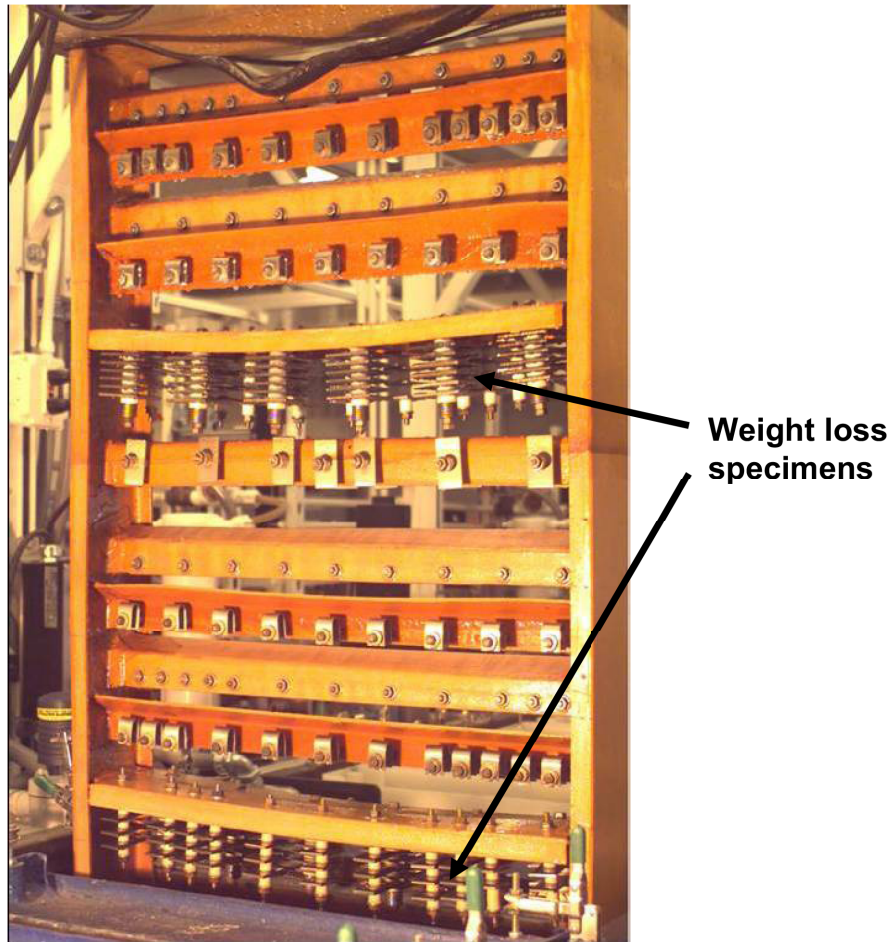


Figure 29. Typical LTCTF corrosion test rack.²⁹

For preparation of the sample for analysis, an area with a large corrosion product cap on the surface was chosen, and the cut was made through this area, which is marked by the red line in Figure 30. This surface corrosion product was located under and adjacent to a Teflon washer as described in the experimental procedure section of the LLNL corrosion paper. Figure 30 shows the area of the test specimen that was prepared for analysis.

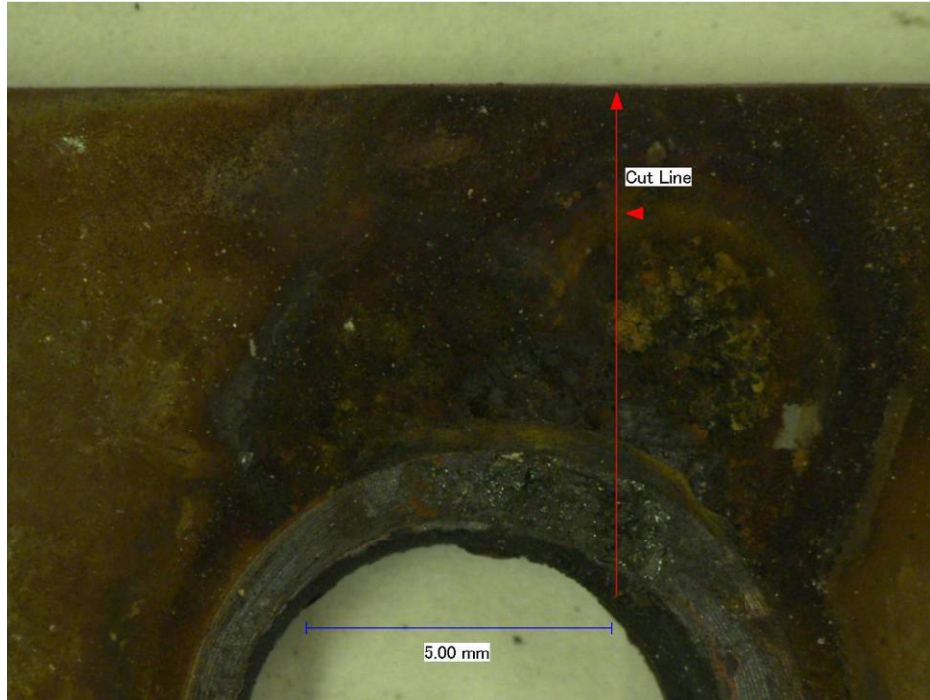


Figure 30. Specimen SSE 30 cut line.

LOM images of the specimen after vacuum mounting are shown in Figures 31 and 32. The sample is totally penetrated under the Teflon attachment washer, with corrosion products evident on the surface and under the original surface.

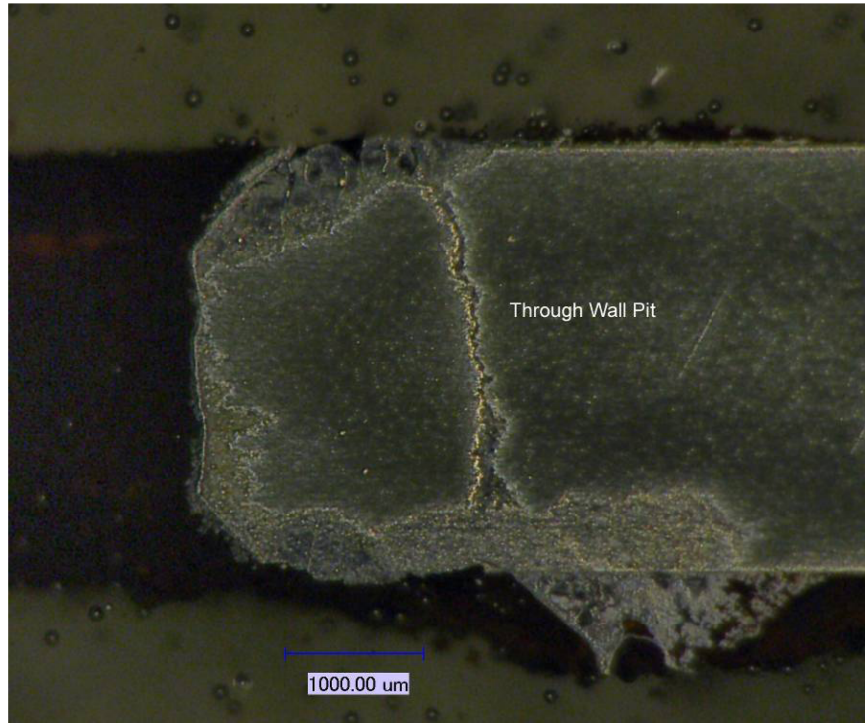


Figure 31. Specimen SSE 30, mounted specimen, showing through-wall penetration and corrosion product.

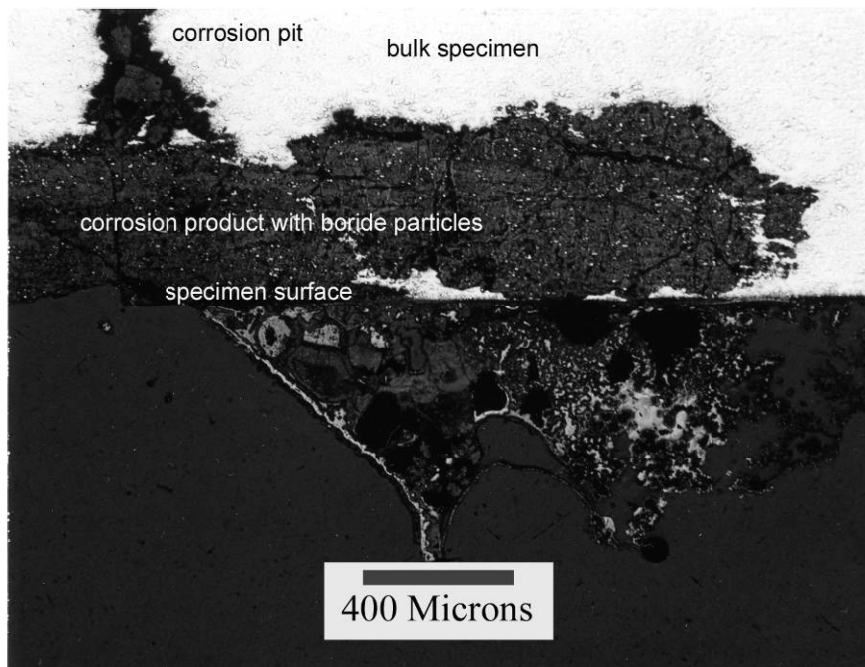


Figure 32. Specimen SSE 30 corrosion products.

Figure 33 shows a SEM SE image of the sampling areas for the corrosion products that lie above and below the original sample surface.

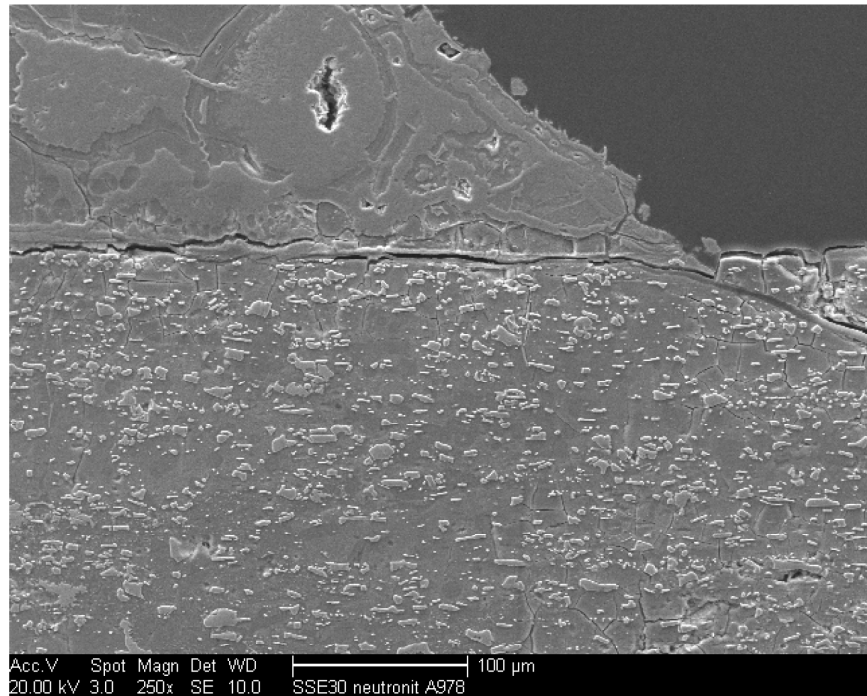


Figure 33. Specimen SSE 30 SE image.

As shown in Figure 34, an area was chosen (box with black border) for sampling in the corrosion product found under the apparent original sample surface. The analytical results are in Table 11. The particles, marked as spots 1 and 2, appear to be borides. Spot 3 has the physical appearance of a boride, but no boron was detected. Spots 4 and 5 are corrosion products where some boron was detected in spot 4 and no boron was detected in spot 5.

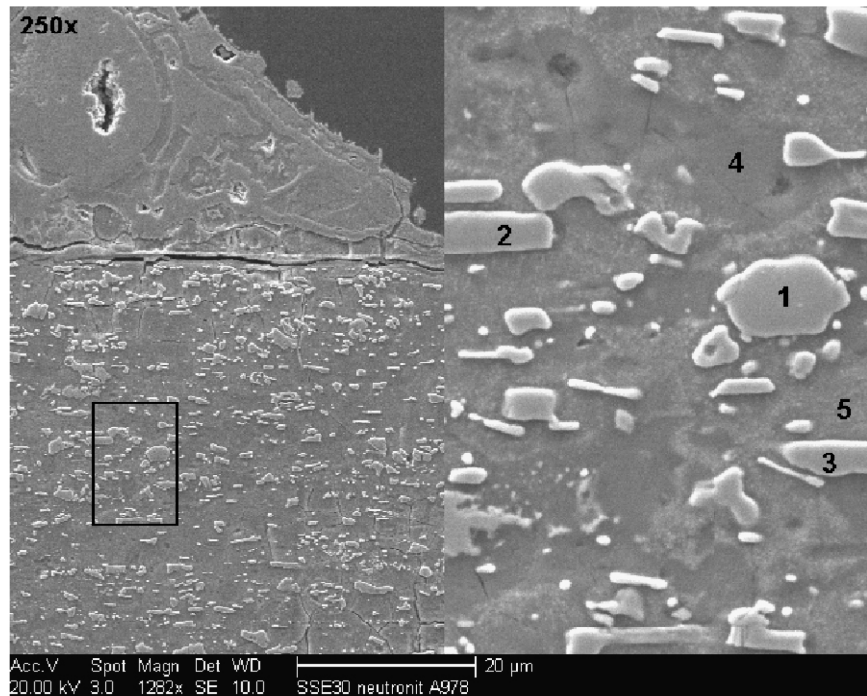


Figure 34. Specimen SSE 30 SE image, corrosion product analysis. (The 20 µm bar corresponds to the image on the right.)

Table 11. Corrosion product analysis, below original surface.

Element	Spot 1	Spot 2	Spot 3	Spot 4	Spot 5
B	1.84	2.02	0.00	1.32	0.0
C	0.62	0.70	0.00	0.99	0.68
O	2.81	2.74	2.67	32.72	37.43
Mo	2.93	2.80	3.06	14.20	13.87
Cr	47.25	48.56	49.85	38.96	38.05
Mn	0.98	1.15	1.24	0.24	0.16
Fe	42.76	41.22	42.16	6.68	4.85
Ni	0.80	0.81	0.97	4.15	3.94
Cu	0.00	0.00	0.06	0.75	1.04

The sample area shown in Figure 35 is the corrosion product deposited above the apparent original-sample surface. The analysis results of the sampled areas are shown in Table 12. The sample areas are iron and chromium-corrosion-product oxides in which boron was detected. Boron was found in the four sampled areas of the corrosion product found on the sample surface.



Figure 35. Specimen SSE 30 SE image, corrosion product analysis.

Table 12. Corrosion product analysis, above original surface.

Element	Spot 1	Spot 2	Spot 3	Spot 4
B	2.72	1.31	3.94	1.98
C	1.75	1.24	1.74	1.15
O	31.27	29.90	29.09	30.69
Mo	2.36	6.15	4.88	2.60
Cr	6.91	7.72	50.37	1.68
Mn	0.61	0.70	2.90	0.31
Fe	52.40	52.07	3.74	58.43
Ni	1.86	0.80	3.16	3.01
Cu	0.12	0.11	0.19	0.16

An area of the bulk metal (unetched) below the corroded surface is shown in Figure 36. The analysis results for the sampled areas are shown in Table 13. The secondary-phase particle sampled at spot 1 is a boride, and spots 2 and 3 correspond to the chemistry of the base austenitic structure of this alloy. Spot 3 does identify boron, but this value may be from borides adjacent or underneath the sampled area being measured by the beam.

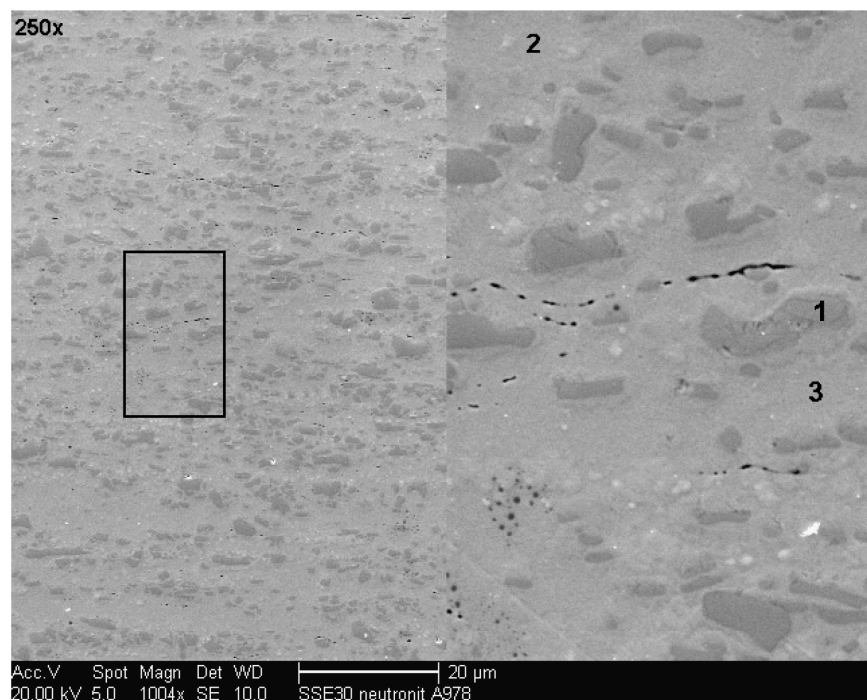


Figure 36. Specimen SSE 30 SE image, bulk metal boride analysis. (The 20 μm bar corresponds to the image on the right.)

Table 13. Specimen SSE 30, bulk metal analysis.

Element	Spot 1	Spot 2	Spot 3
B	2.47	0.00	1.67
C	1.49	0.38	0.75
O	2.77	1.41	1.40
Mo	4.58	1.68	1.53
Cr	39.25	11.22	11.07
Mn	3.99	2.25	2.09
Fe	38.53	68.67	67.62
Ni	3.28	13.52	13.32
Cu	3.65	0.87	0.55

4.1.4 Analysis of Corrosion Product from Neutronit Specimen SSE2 from the LTCTF

A loose sample of the corrosion product in the storage bag of sample SSE-02 was collected and analyzed by XRD. Sample SSE-02 is a Neutronit A978 sample (Heat E084295 in Table 1), which was exposed in the vapor space to simulated acidified water at 90°C for 2,134 days at the LTCTF.¹³ The results show that the corrosion product consists mainly of FeO(OH) (goethite) and Fe₂O₃ (hematite) with no evidence of crystalline borides being present.

5. CONCLUSIONS

Corrosion testing of five neutron-absorbing alloys, Type 304B4 Grade A, Type 304B5 Grade A, Type 304B6 Grade A, Neutronit A978, and Ni-Cr-Mo-Gd alloy, was performed using electrochemical testing methods. One test sequence compared the performance of two different heats of a Ni-Cr-Mo-Gd with the Ni-Cr-Mo alloy specified for the waste package outer barrier (Alloy 22).

The conditions were based on those expected for a waste package, should the outer barrier breach and the internals be exposed to moisture. PD tests were performed to determine the localized characteristics of the materials. Measurement of the E_{corr} was used to determine the equilibration potentials under aeration to determine values for performing PS tests. The PS tests hold the potential of the specimen at a value, as determined from the E_{corr} testing while measuring the current. The current from this test can be used to determine the corrosion rate and/or propensity toward localized corrosion. In addition, LPR tests were performed as a second method to determine the corrosion rate. Damage to the specimens was observed using photography, LOM, and SEM.

While acceptable results were obtained for 304B4 and Ni-Cr-Mo-Gd alloys, experimental problems occurred for the A978 alloy in PS tests. These problems stemmed from having to adapt long-term exposure test specimens to electrochemical testing. The problem was due to the method used for specimen contact.

The testing performed on these neutron absorbers has shown behavior that contradicts some of the previous work on these types of alloys.^{13,30} However, in those previous tests the conditions are more aggressive (temperature, pH, ionic content, etc.) than those used here. The tests here contain very low ionic contents and/or moderate pH values, as defined in the Technical Work Plan.¹⁹ Very passive conditions were observed for the 304B4 SS in all cases. There was evidence of metastable pitting on the borated stainless steel, though sustained pitting events were not observed. Several 304B4 specimens showed significant but isolated damage under the crevice formers. It is difficult to determine if the corrosion occurred prior to the PS tests, particularly during aeration where the potentials were fairly positive on the specimens that may not yet have been fully passivated. Some further investigation of this observation is warranted. Ideally, the tests would extend conditions such that the localized corrosion initiation threshold in potential, temperature, and solution composition (Cl/NO₃ ratio, pH) are known.

The results of the Ni-Cr-Mo-Gd alloy tests, compared to the borated stainless steel alloys, are less clear. The measured corrosion current for the Ni-Cr-Mo-Gd alloy was higher than that measured for the 304 B4 stainless steels, but the current, in this case, was measuring the dissolution of the secondary phase (gadolinide) for the Ni-Cr-Mo-Gd material. Therefore, the initial corrosion rate for the Ni-Cr-Mo-Gd material is determined by the very reactive gadolinide secondary phase.³¹ This apparent general-corrosion rate was several orders-of-magnitude higher than for the 304B4, Grade A material. The secondary-phase (FeCr)₂B of the borated stainless steel appears to be stable, likely due to the high Cr content; thus, it does not contribute to the corrosion directly. This secondary phase (boride) is known to reduce the overall localized corrosion properties due to chromium depletion from the austenite phase adjacent to the boride.^{10,13,27} Evidence shows that the gadolinide phase was not fully removed in these tests; thus, the final PS corrosion current values (and calculated corrosion rate) are affected by continued corrosion of the gadolinide phase. It is anticipated that the general corrosion performance would improve after the full removal of this phase and would approach the performance level of Alloy C-4 or Alloy 22, depending on the particular chromium level of the heat being tested. As shown in previous work, the primary austenitic phase of the Ni-Cr-Mo-Gd alloy was very resistant to localized corrosion. The localized corrosion resistance benefits of the Ni-based alloy would be useful for more aggressive conditions than those that were tested in this study. In any case, long-term corrosion testing needs to be performed to verify the results of these preliminary tests.

Additional work should be performed to determine a rate for the loss of boron during localized corrosion of 304B4, Grade A stainless steels. Boride dissolution by the in-package solution or capture in a corrosion product should also be investigated further.

6. REFERENCES

1. ASTM A887-89, "Standard Specification for Borated Stainless Steel Plate, Sheet, and Strip for Nuclear Application," American Society for Testing and Materials, 2004.
2. K. Wasinger, "High Density Spent Fuel Storage in Spain-Capacity for the Entire Life," *Nuclear Plant Journal*, July-August 1993, p. 46.
3. D.G. Abbott and R.E. Nickell, "Experience with Certifying Borated Stainless Steel as a Shipping Cask Material," *1st International Topical Meeting on High-Level Radioactive Waste Management, Las Vegas, NV, April 1990*.
4. Waste Package Neutron Absorber, Thermal Shunt, and Fill Gas Report, B00000000-01717-2200-00227 REV 00, January 2000.
5. ASTM B932-04, *Standard Specification for Low-Carbon Nickel-Chromium-Molybdenum-Gadolinium Alloy Plate, Sheet, and Strip*, American Society for Testing and Materials, 2004.
6. DOE/SNF/REP-011, *Preliminary Design Specification for Department of Energy Standardized Spent Nuclear Fuel Canisters*, Department of Energy, Volume I - Design Specification, Revision 3, August 17, 1999.
7. Quality Assurance Requirements and Description, DOE/RW-0333P, Revision 18, DOC.20060602.0001, 10/02/2006.
8. Electrochemical Corrosion Testing of Borated Stainless Steel Alloys, INL/EXT-07-12633, May 2007.
9. H.J. Goldschmidt, "Effect of Boron Additions to Austenitic Stainless Steels Part II, Solubility of Boron in 18% Cr, 15% Ni Austenitic Steel," *Journal of the Iron and Steel Institute*, November 1971, p. 910.
10. J.W. Martin, "Effects of Processing and Microstructure on the Mechanical Properties of Boron-Containing Austenitic Stainless Steels," *Proceedings Symposium Waste Management, University of Arizona, AZ, 1989*, p. 293.
11. ASME Boiler and Pressure Vessel Code, Section III, Division 1, Case N-510-1, "Borated Stainless Steel for Class CS Core Support Structures and Class 1 Component Supports," December 12, 1994
12. ASME Boiler and Pressure Vessel Code, Section III, Division 3, Case N-728, "Use of B-932-04 plate material for non-pressure retaining spent-fuel containment internals to 650F (343C), Section III, Division 3," May 10, 2005.
13. D.V. Fix, J.C. Estill, L.L. Wong, and R.B. Rebak, "General and Localized Corrosion of Austenitic and Borated Stainless Steels in Simulated Concentrated Ground Waters," *American Society of Mechanical Engineers Pressure Vessels and Piping Division (ASME-PVP) Conference, San Diego, CA, July 2004*.
14. INL DWG 630285, "Crevice Corrosion Specimen," March 15, 2005.
15. Kevin Mon (YMP), (Kevin_Mon@ymp.gov), "Fw: PD," to Ted Lister (INL), (Tedd.Lister@inl.gov), July 24, 2006.
16. PLN-1880, "Experimental Plan for Electrochemical Corrosion Testing of Ni-Cr-Mo-Gd Alloys," Rev. 1, July 13, 2005.
17. PLN-1885, "Experimental Procedures for Corrosion Testing of Ni-Cr-Mo-Gd Alloys," Rev 2, September 1, 2005.

18. ASTM G5-94, "Standard Reference Test Method for Making Potentiostatic and Potentiodynamic Anodic Polarization Measurements," American Society for Testing and Materials, 2004.
19. Sandia National Laboratory, Technical Work Plan for Borated Stainless Steel Testing, DOC.20070206.002, January 2007.
20. C.V. Robino and M.J. Cieslak, "High Temperature Metallurgy of Advanced Borated Stainless Steels," *Metallurgical and Materials Transactions A*, vol. 26, 1995, p. 1673.
21. ASTM G102-89, "Standard Practice for Calculation of Corrosion Rates and Related Information from Electrochemical Measurements," American Society for Testing and Materials, 2004.
22. BSC (Bechtel SAIC Company), "General and Localized Corrosion of the Waste Package Outer Barrier," Las Vegas, Nevada, 2004.
23. ASTM G59-97, "Standard Practice for Conducting Potentiodynamic Polarization Resistance Measurements," American Society for Testing and Materials, 2003.
24. A.J. Bard and L.R. Faulkner, *Electrochemical Methods*, 2nd ed., Wiley, New York, 2001, Chapter 3.
25. D.C. Silverman, *Uhlig's Corrosion Handbook*, 2nd ed., Wiley, New York, 2000, pp. 1197-1198.
26. Electrochemical Corrosion Testing of Neutron Absorber Materials, INL/EXT-06-11772, November 2006.
27. E.A. Loria and H.S. Isaacs, "Type 304 stainless Steel with 0.5% Boron for Storage of Spent Nuclear Fuel", *Journal of Metals*, December 1980, p. 10.
28. A. Kugler, Neutronit A976, Sheet and Plate for Nuclear Engineering, Bohler Bleche GmbH, September 1997.
29. D.V. Fix and R.B. Rebak, "The Long Term Corrosion Test Facility at the Lawrence Livermore National Laboratory," UCRL-Proc-229377, Lawrence Livermore National Laboratory, Livermore, CA. 94550, March 34, 2007.
30. D.A. Moreno, B. Molina, C. Ranninger, F. Montero, and J. Izquierdo, "Microstructural Characterization and Pitting Corrosion Behavior of UNS S30466 Borated Stainless Steel," *Corrosion* 60 (2004) 573.
31. T.E. Lister, R.E. Mizia, P.J. Pinhero, T.L. Trowbridge, and K.B. Delezene-Briggs, "Studies of the Corrosion Properties of Ni-Cr-Mo-Gd Neutron-Absorbing Alloys," *Corrosion*, vol. 61, 2005, p. 706.

Appendix A
A978 PS Test Data

Appendix A

A978 PS Test Data

This supplemental report provides data from tests of A978 specimens. These tests were not included in the main report due to experimental issues with the design of the specimen electrical contact. Two methods were used to make the specimen contact to the non-standard specimens. Specimens for Tests 072706 and 080206 were attached using short platinum wire spot-welded to a corner of the coupon and a longer plastic insulated wire soldered to that wire. Then the entire exposed wire was insulated using Dexter Hydrosol epoxy. Problems were noted during the testing with delamination of the epoxy, leading to corrosion of the wire and solder. With these tests, the initial part of the experiment (E_{corr} measurement, LPR) is likely not affected. However, the PS data is likely affected. It is not known when the delamination affected the test, so the data is of limited use. A second attachment method used a platinum wire (corrosion resistant, but not unreactive) spot welded to a corner of the coupon and extended out of the cell. No coating was used, which left the platinum wire and spot-weld damage exposed to the solution. Tests 082206 and 082806 used this contact, which was stable, but the platinum wire was exposed; thus, it could contribute to the measured current. Table A1 (page 55) shows data tabulated from PS testing of A978 specimens.

Figures A1 and A2 show the E_{corr} measurement for the A978 tests under aerated and N_2 purge. There does not appear to be a consistent common behavior in the E_{corr} data except of the two epoxy coated specimens under N_2 purge.

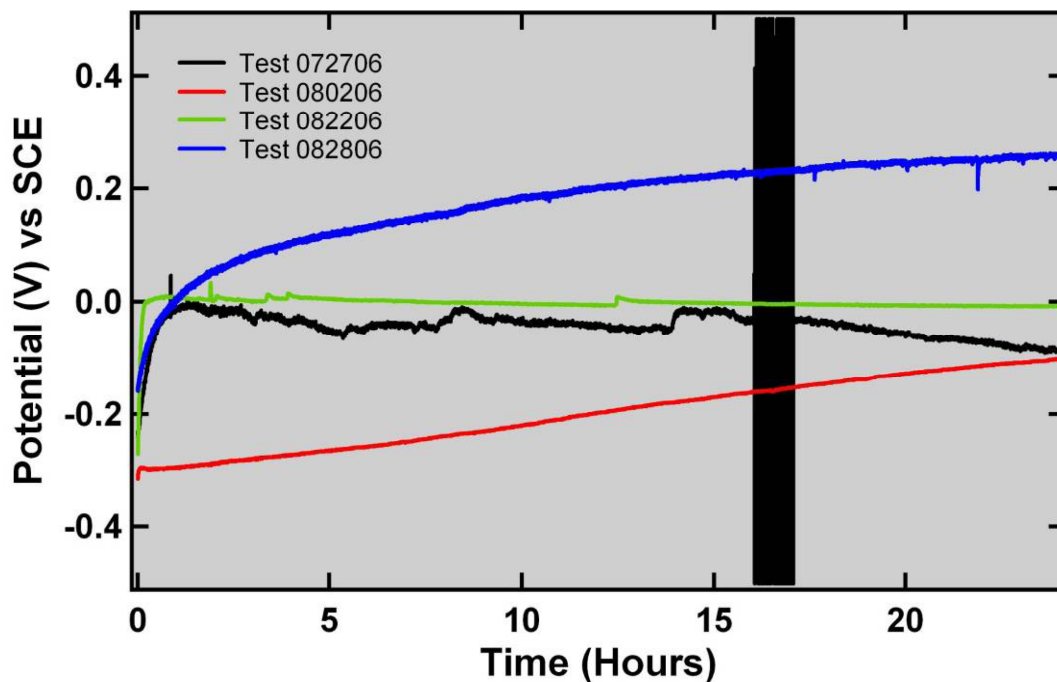


Figure A1. Plots of E_{corr} versus time for A978 specimens with aeration.

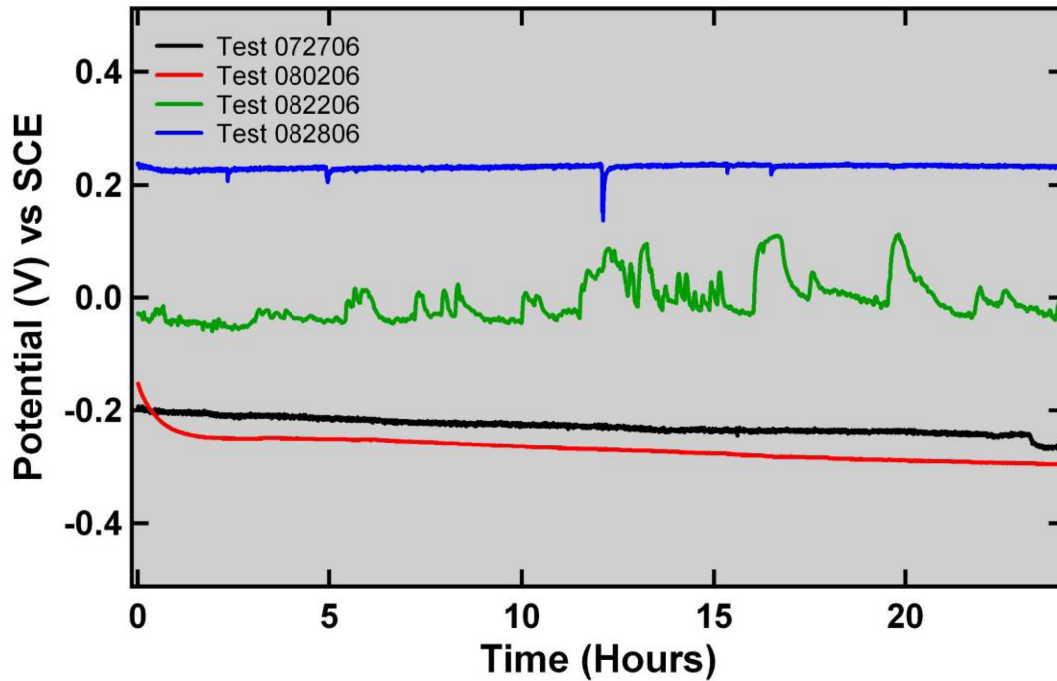


Figure A2. Plots of E_{corr} versus time for A978 specimens during N_2 purge.

Figure A3 shows the PS data obtained from the four A978 specimens. The two specimens using an epoxy coating have much higher current. After examination of the specimens after the test (see Figure A4), it was noticeable that the contact to the specimens was corroded. The specimens using only a bare, platinum-wire contact showed low negative currents with a short positive current excursion due to localized corrosion. This negative current is evidently due to the exposed platinum wire and is likely an electrochemical reaction with dissolved species. Thus, in all cases a corrosion rate cannot be ascertained because the current is dominated by other reactions at the contact wires. Because the net current was negative, this suggests that the anodic corrosion current for the A978 was low.

Figure A4 shows macro photographs of the specimen surfaces after testing. While the electrochemical data was not very useful, the damage to the surface observed during the test is likely to be what would occur on a test using the properly configured crevice specimen. The exception might be Test 072706. The contact was so corroded that the specimen was not in electrical contact for much of the test. A thick brown film coated the surface of the Test 072706 specimen, and the solution was clouded with precipitate. The film appeared to be from the corrosion of the solder and wire of the contacting lead. Significant crevice corrosion was observed only on Tests 080206 and 082206. LOM of damage to these specimens under the crevice formers is shown in Figure A5. There was no significant damage to Test 072706 and 082806 specimens.

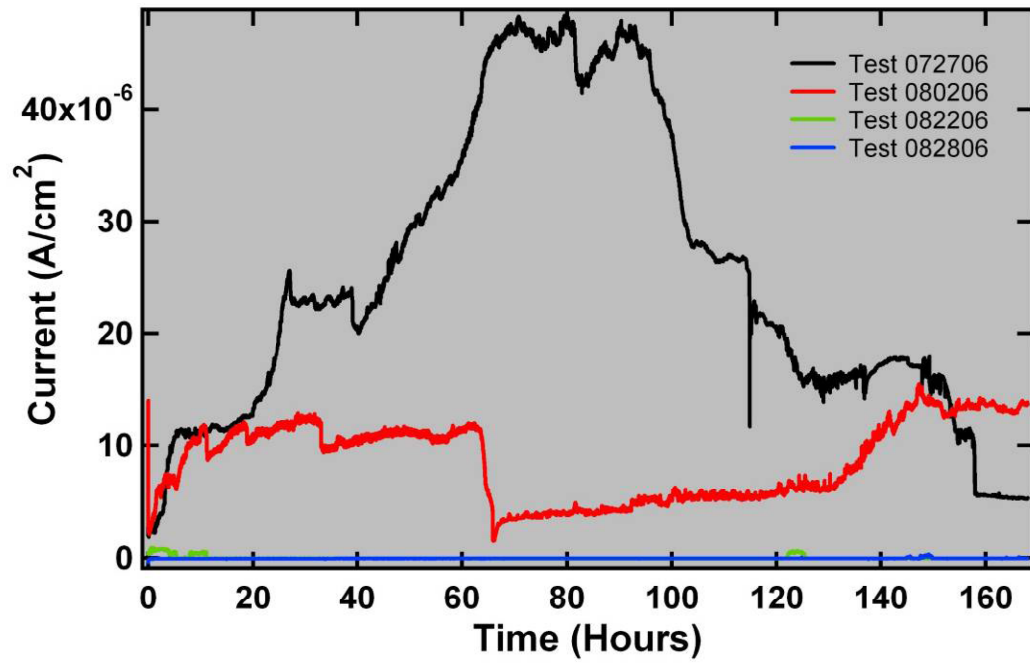


Figure A3. Plots of current versus time for PS tests of A978 specimens.

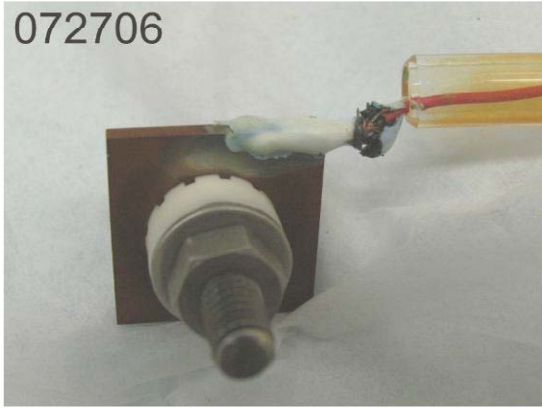


Figure A4. Macro photographs of A978 specimens after testing. Note that part of the platinum wire from the Tests 082206 and 082806 remains in the corner of these specimens.

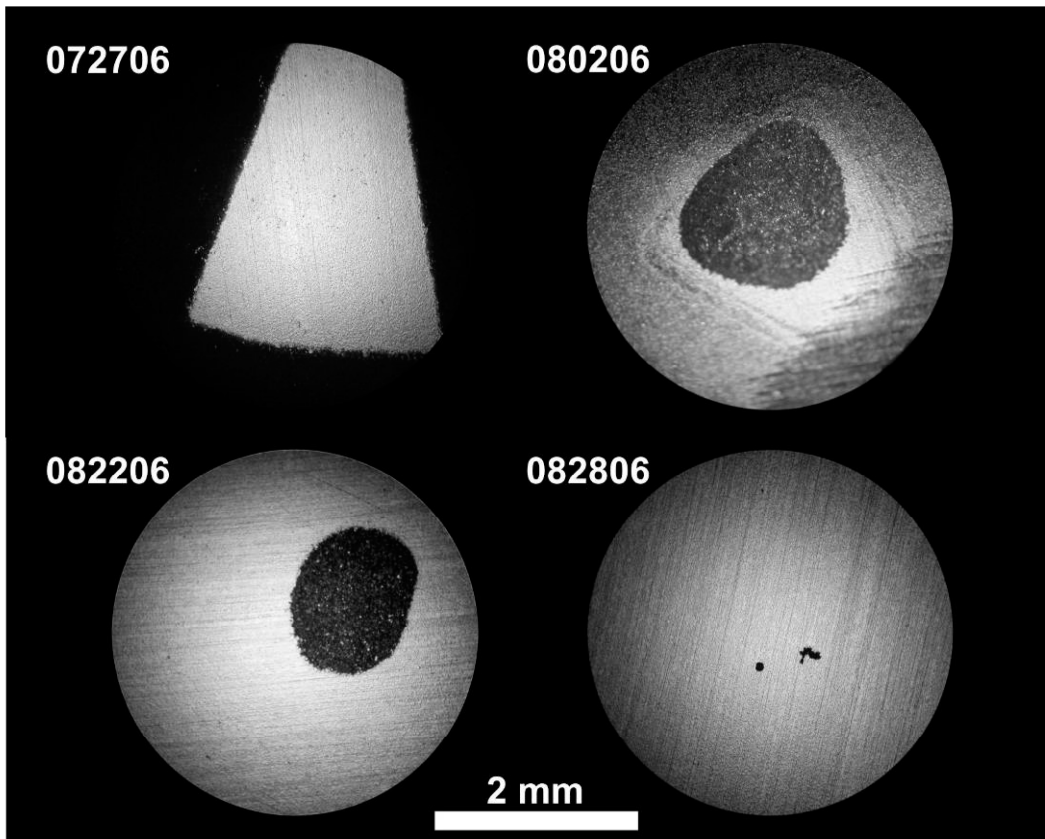


Figure A5. LOM images of A978 specimens after testing.

Table A1. Data for A978 tests.

Test ID	Solution	Final E_{corr} Ox (V)	Final E_{corr} N_2 (V)	LPR CR ($\mu\text{m}/\text{yr}$)	Total Charge (C/cm^2)	Peak Current (A/cm^2)	I_{corr} (A/cm^2)	CR ($\mu\text{m}/\text{yr}$)	EC Test Comments	Solution Observations	Sample Observations
072706	B1	-0.092	-0.265	0.975	14.94	4.82E-05	5.32E-06	52.7	Ox E_{corr} smooth except for one very erratic period, N_2 E_{corr} fairly smooth, bad contact	Orange/Brown with precipitates	Orange film from corrosion of contact, no crevice corrosion
080206	B3	-0.102	-0.2951	1.04	5.22	1.55E-05	2.11E-04	135	E_{corr} smooth, PS very erratic and choppy, bad contact	Clear and colorless	One large crevice pit area
082206	B1	-0.0078	-0.0018	0.657	7.14E-03	9.49E-07	-2.54E-08	N/A	Some pit initiation, negative PS current, interference with platinum	Clear and colorless	Crevice corrosion evident
082806	B3	0.259	0.233	0.196	-0.01409	3.16E-07	-2.22E-08	N/A	Some pit initiation, negative PS current, interference with platinum	Clear and colorless	No crevice corrosion

Note: Tests 072706 and 080206 had corrosion of the specimen contacts leading to excessive currents in the PS tests

Tests 082206 and 082806 had negative i_{corr} values and thus corrosion rate was calculated